Proceedings of the International Association for Shell and Spatial Structures (IASS) Symposium 2009, Valencia
Evolution and Trends in Design, Analysis and Construction of Shell and Spatial Structures
28 September – 2 October 2009, Universidad Politecnica de Valencia, Spain
Alberto DOMINGO and Carlos LAZARO (eds.)

Numerical study on effect of member length error on structural properties of single layer pin-jointed grid dome composed of wooden truss system

Masumi FUJIMOTO*, Shinichiro KATAYAMA[a], Tomoichiro KANAME[b], Katsuhiko IMAI[c] and Takahiro MACHINAGA[a]

*Dep. Urban Engineering, Graduate School of Engineering, Osaka City University, Sugimoto 3, Sumiyoshi-ku, Osaka, 558-8585, Japan
E-mail:fujimoto@arch.eng.osaka-cu.ac.jp

[a] Takenaka corporation
[b] Taisei corporation
[c] Osaka university

Abstract

This study examines a single layer three-way pin-jointed grid dome constructed from of wooden truss system. We show the effect of the member length error on the initial imperfection and nodal buckling behavior by the numerical analysis results considering geometrical nonlinearity. In numerical calculation, the member length errors are assumed to be a normal distribution. The distribution and magnitude of the initial axial force and displacement are evaluated with respect to the mean and SD (standard deviation) of the member length errors. The range of the initial imperfection and the tolerance of manufactured member length are also predicted by the mean and SD of the numerical results. The properties of nodal buckling load and buckling mode are also discussed. The nodal buckling load is mainly affected by the SD of member length error and the effect of mean of member length error on the buckling is secondary. When SD of member length error changes from zero to 0.10 cm, the mean of the nodal buckling load decreases by about 50 % and the area of nodal buckling mode changes from the overall dome to the inner region.

Keywords: single layer three-way grid dome, thin round timber, member length error, pin-jointed member, initial imperfection, nodal buckling load

1. Introduction

Single layer grid domes are used as the structural system to cover the large span. It has been reported that the buckling load of single layer grid domes is reduced by the initial imperfections of configuration and the initial stress, as in AIJ [1].

To promote forestry thinning, we have proposed a prefabricated truss system with thin round timber. We have already applied this truss system to a single layer grid dome, a single layer cylindrical roof grid shell, and tensegrity structures, as in Fujimoto et al. [4], [5],[6],[7],[8],[9]. When a prefabricated truss system using thin round timber is applied to spatial frame structures, it is expected that member length error, the variation in elastic modulus of the wooden members and the initial crookedness of members influence the buckling load of single layer grid shells.

In studies of the effects of initial imperfections on the buckling load, the initial configuration imperfections are almost specified by the deterministic method based on the buckling mode or the randomly assumed distribution. For example, the relations between buckling load and configuration parameters of a single layer grid dome are calculated corresponding to the various assumed configuration imperfections, as shown in Ogawa et al. [11]. There are few studies of the effects of initial imperfections generated by member length error on the structural behavior of a single layer grid shell. The effects of member length error on the initial stress and initial displacement are as reported in Kato et al. [10]. Kato showed that the standard deviation of member length error varies almost linearly with the standard deviation of initial axial force, etc. As far as we know, the effect of member length error on the buckling load of a single layer grid shell was not reported.

In this study, we examine a single layer three-way pin-jointed grid dome constructed as a prefabricated wooden truss system. The member length error is attracted among the imperfection expected in a prefabricated wooden truss system. The structural behavior of a single layer pin-jointed grid dome is examined here with the numerical study considering geometrical nonlinearity. In numerical calculations, the member length error is set to vary in a normal distribution by Box Muller method. The effect of member length error on configuration imperfection, initial axial force, and nodal buckling behavior are discussed.

2. Outline of numerical analysis

2.1. Analysis model

The overall configuration of a single layer three-way pin-jointed dome is shown in Figure 1. The dome plan is a hexagon composed of equilateral triangles. The surface of the dome is determined by the vertical projection of the nodes onto a spherical surface. The radius of curvature is 6000 mm and the half open angle subtended by the dome is 30°. The plan and elevation are shown in Figure 2. The constituent members are round timbers of Japanese cypress. Member diameter is 6.0 cm; elastic modulus of member 1000 kN/cm^2. The boundary condition of the dome is that all peripheral nodes of the dome are pin supported. The applied load is the uniform nodal gravity load.

2.2. Analysis method

The member model is a pin-jointed truss member excluding joint size. The load incremental method considering the geometrical nonlinearity is used to calculate the initial imperfection by member length error as shown in Fujimoto [3] and the equilibrium path from the zero load state to the buckling load. Member buckling is not considered in this analysis.

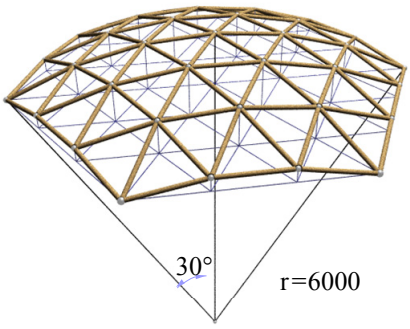

Figure 1: Overall configuration

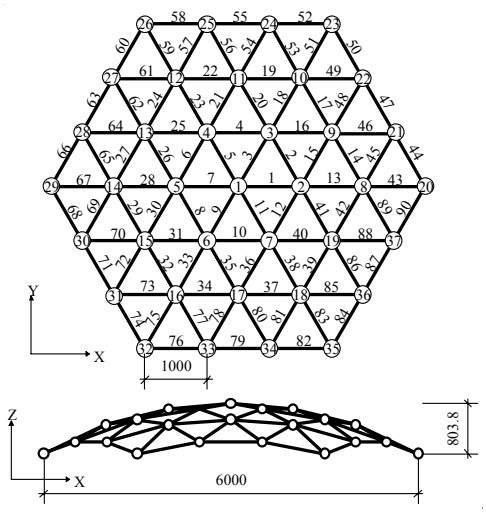

Figure 2: Plan and elevation

2.3. Determination of member length error

The member length error is predicted to be a random variable and is assumed to follow a normal distribution. The distribution of member length error is determined by Box Muller method. The magnitude of member length error is determined by the manageable tolerances as in AIJ recommendation [2] and some values for member errors obtained by experimental study, as in Fujimoto [9]. In this study, the means of member length error are 0.0, ±0.01, ±0.02, ±0.03, ±0.04, and ±0.05 cm. The standard deviations are 0.0, 0.01, 0.02, 0.03, 0.04, 0.05, 0.07, and 0.1 cm. Eighty eight cases are considered for both mean value and standard deviation. Two hundred samples are used for each combination.

3. Initial imperfection

3.1. Initial axial force

Figure 3 shows the relation between the mean of the initial axial force on each member in the ring direction and the SD (standard deviation) of member length error. In these Figures, the mean values of member error are zero, ±0.03, and ±0.05 cm. In the following Figures, the numerical results are based on 200 sample cases with the SD of member length error not equal to zero. Figure 4 shows the initial axial force on a member in the radial direction. The mean of the initial axial force increases with increasing SD of member length error, but is very much smaller than the SD of the initial axial force. Figure 5 shows the relation between the SD of the initial axial force and the SD of member length error. As shown in Figure 5, it is confirmed that the SD of the initial axial force is proportional to the SD of member length error. The mean of the initial axial forces on members in the inner region is

dominated by the SD of the member length error. However, the mean of the initial axial forces on a member in the peripheral area is determined by the mean and SD of the member length error.

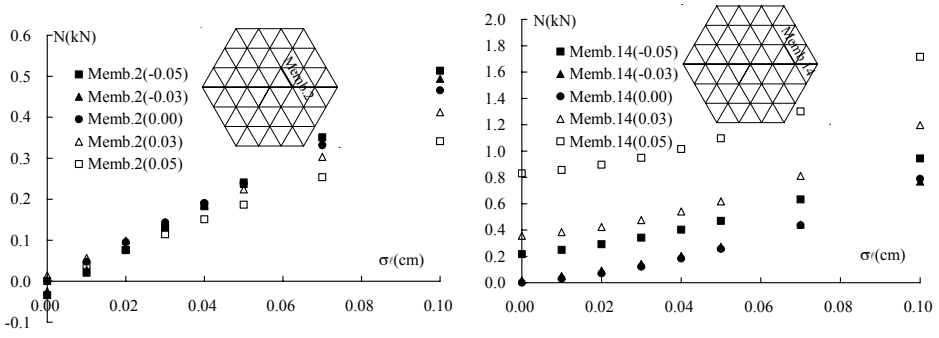

Figure 3: Mean of the initial axial force on members in the ring direction

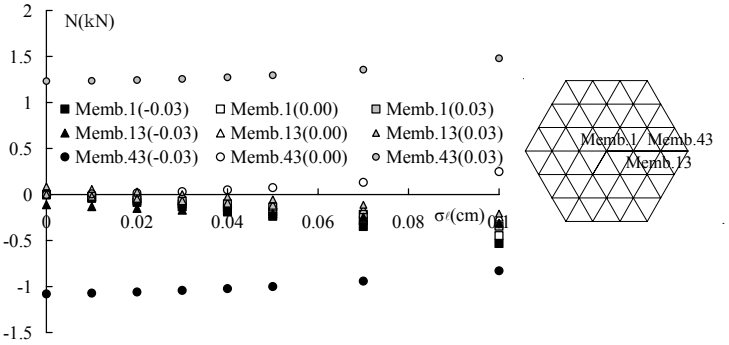

Figure 4: Mean of the initial axial force on members in the radial direction.

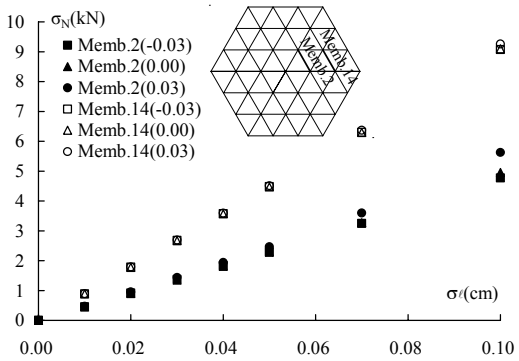

Figure 5: SD of the initial axial force on members in the ring direction

Figure 6 shows the frequency distribution of the initial axial force on member 2 for the case of (0.00-0.10). The first number, 0.00 cm, denotes the mean member length error and the second number, 0.10 cm, denotes the SD of member length error. The curve in this figure denotes the normal distribution approximation of the samples. As shown in this Figure, the distribution of initial axial forces follows the normal distribution when the member length error follows a normal distribution.

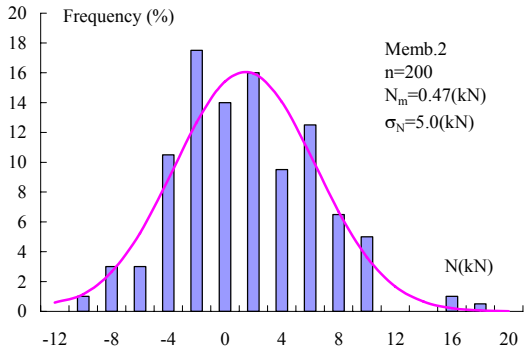

Figure 6: Frequency distribution of the initial axial force on member 2(0.00-0.10)

3.2. Distribution of initial axial force

Figure 7 shows the initial axial force distribution for a member length error of 0.03 cm. The SD of member length errors are 0.0, 0.02, and 0.10 cm. The result for a member length error of -0.03 cm is also shown. The distribution of the initial axial force is uniform in the inner region for lower SD of member length error and forms a partial pattern with larger SD.

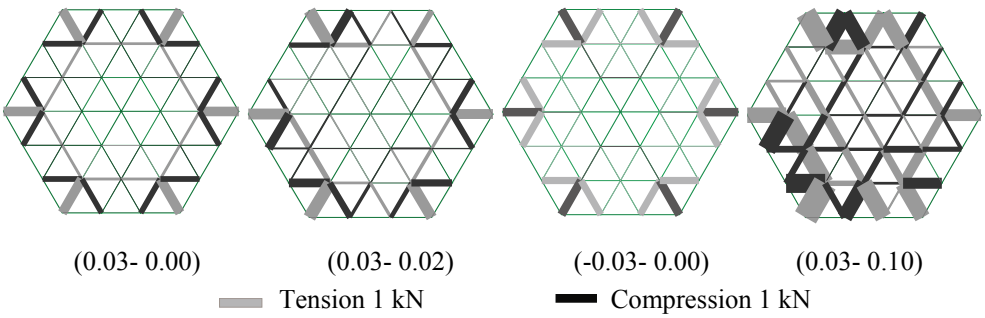

Figure 7: Initial axial force distributions

3.3. Initial nodal displacement

Figure 8 shows the nodal displacement in the z direction. In this Figure, the square, triangle and circle denote nodes 1, 2, and 8 respectively. The black, open and gray marks represent

member length errors of -0.03, 0.0, and 0.03 cm respectively. Figure 9 shows the SD of the z direction displacement of nodes in the radial direction.

As shown in Figure 8, the mean z direction displacement is positive (negative) when the member length error is positive (negative) and is almost constant even when there is an increase in the SD of member length error. The mean of nodal displacements in the z direction is proportional to the mean member length error. As shown in Figure 9, the SD of the z direction displacement is not affected by the member length error and is proportional to the SD of the member length error. As shown in Ogawa et al. [11], the amplitude of the configuration imperfection, δ, is usually assumed to be $0.2t_e$, in which t_e denotes the equivalent shell thickness. In this model, the amplitude $0.2t_e$ is 1.04 cm. For example, for values of (0.03-0.07), the mean nodal displacement in the z direction, 0.2, plus 2xSD of the nodal displacement in the z direction, 0.4 cm, the nodal imperfection in the z direction ranges from -0.6 cm to 1.0 cm. For the values (-0.03-0.07), the nodal imperfection ranges from -1.0 cm to 0.6 cm. This suggests that (0.03-0.07) and (-0.03-0.07) are examples of tolerances of manufactured member lengths and the SD of the manufactured member length that keep the nodal imperfection within the allowable range.

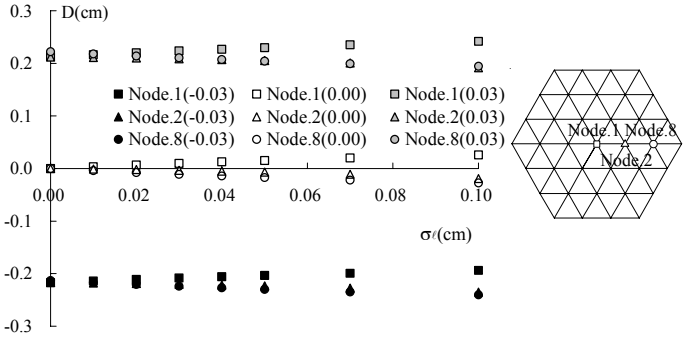

Figure 8: Mean of z directional displacement in nodes along a radial direction

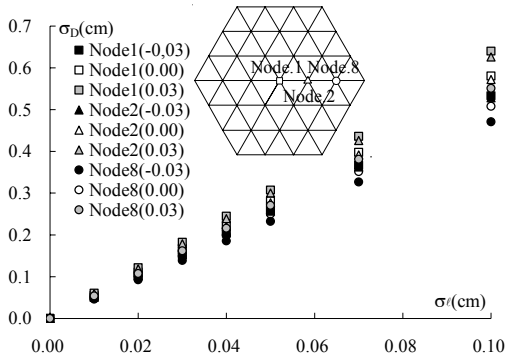

Figure 9: SD of z direction displacement in nodes along a radial direction

Figure 10 shows the frequency distribution of the z direction displacement of node 1(0.00-0.10). As shown in the initial axial force, the z direction displacement is also fitted to a normal distribution.

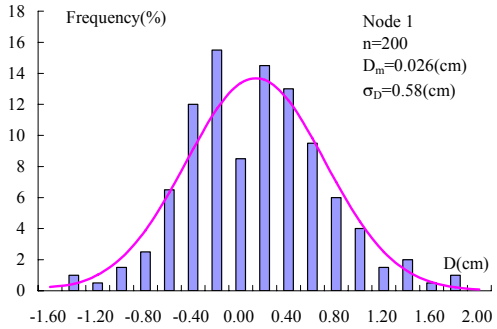

Figure 10: Frequency distribution of the z direction displacement of node 1

Figure 11 shows both the z direction displacement of node 2 and the x direction displacement. Measured against the z direction displacement, the x direction displacements are about 20 % and the y direction displacement about 2 %. In the comparison between the experimental and numerical results for a single layer shallow grid dome, we had already used the measured values as the node level in the z direction to consider the configuration imperfection. This approximate treatment is a significant process in engineering.

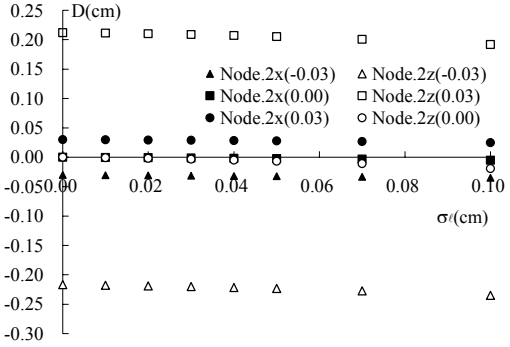

Figure 11: x and z direction displacements of Node 2

Figure 12 shows the initial displacement image of the dome meridian. The dotted line is the original position and the solid line denotes the initial displacement image of nodes in the meridian. The configurations of a single layer gird dome with positive member length error are upward displacements and those with negative member length error are downward displacements.

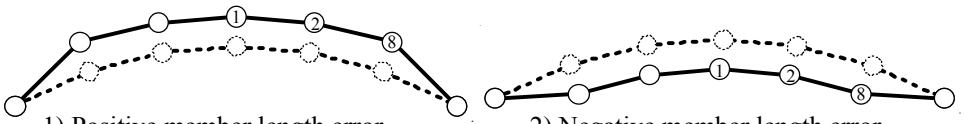

1) Positive member length error 2) Negative member length error

Figure 12: Deformation image corresponding to member length error

4. Nodal buckling behavior

4.1. Nodal buckling load

Figure 13 shows the relation between nodal buckling load and the SD of member length error. Figure 14 shows the relation between nodal buckling load and the mean of member length error. In Figures 13 and 14, the nodal buckling load is expressed in P_{cr} / P_{cr}^{E}. P_{cr} denotes the nodal buckling load and $P_{cr}^{E} (= 33.7\text{kN})$ denotes the nodal buckling load of a single layer grid dome without initial imperfection. As shown in Figure 13, the nodal buckling load decreases, corresponding to the increase in the SD of the member length error. If the SD of the member length error is equal to 0.1 cm, the nodal buckling load of a grid dome with imperfection is 50 to 60 % of that of a grid dome without imperfection.

As shown in Figure 14, when the SD of member length error ranges from zero to 0.02 cm, the nodal buckling load decreases, corresponding to the decrease in the mean of the member length error. When the SD of the member length error is more than 0.03 cm, buckling load decreases, corresponding to the increase in the mean of the member length error. When the SD of member length error changes from 0.0 to 0.10 cm, the buckling load is reduced by about 50 %. The effects of mean of member length error on buckling load are smaller than those of SD of member length error. In Figure 14, the red circle denotes a change in buckling mode (ref. Figure 16).

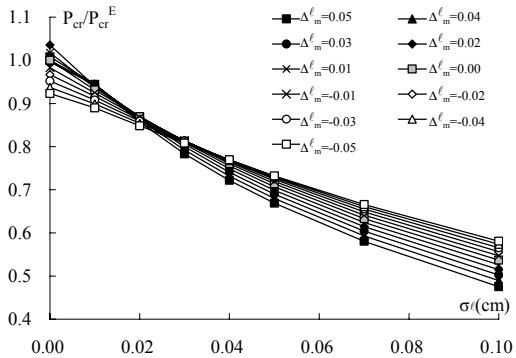

Figure 13: Relation between nodal buckling load and SD of member error

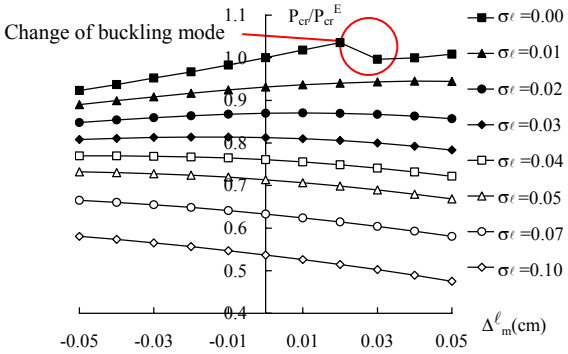

Figure 14: Relation between nodal buckling load and mean of member length error

Figure 15 shows the relation between the SD of the nodal buckling load and the SD of member length error. The SD of the nodal buckling load increases greatly with increasing SD of member length error. But the increase of the ratio of SD of the buckling load gradually decreases as the SD of member length error increases. Figures 14 and 15 show that the buckling load for values of (0.03-007) and (-0.03-0.07) ranges from 15 to 26 kN in terms of mean plus 2xSD. This also shows that the nodal buckling load is mainly affected by the SD of the member length error.

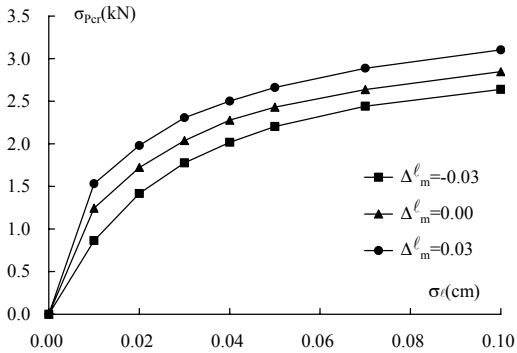

Figure 15: Relation between SD of nodal buckling load and SD of member length error

4.2 Nodal buckling mode

Figure 16 shows examples of nodal buckling modes. When the mean and SD of the member length error are small, the frequency of the nodal buckling of the overall dome surface is larger than that of nodal buckling in local areas. It is guessed that the imperfection distribution of node level is so small that the distribution of member axial forces is uniform.

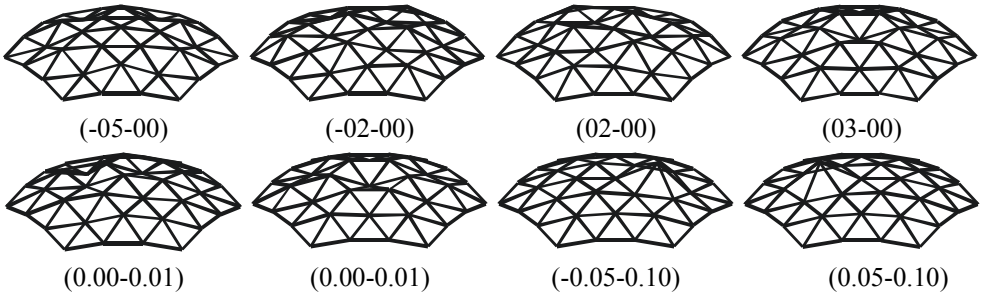

Figure 16: Example of nodal buckling mode

Figure 17 shows the SD of normal nodal displacement mode in the z direction. The original component of the nodal displacement mode is normalized by the square root of the sum of squares of all components of the displacement mode.

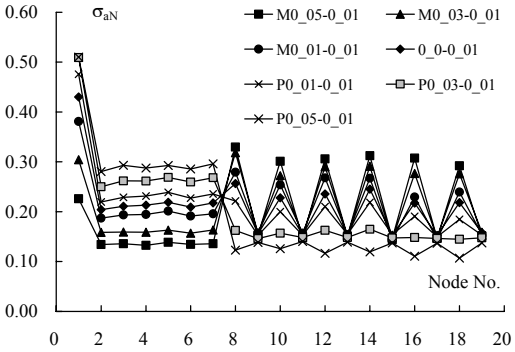

1) SD of member length error is 0.01 cm

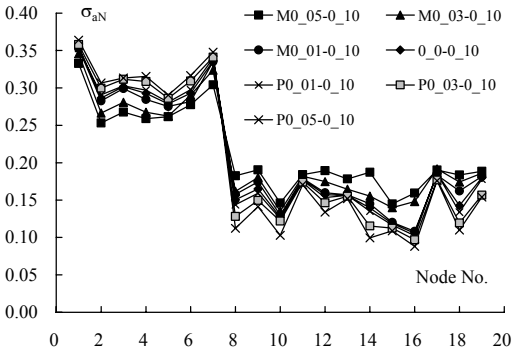

2) SD of member length error is 0.10 cm

Figure 17: SD of node amplitude of buckling mode

When the SD of the member length error is 0.01 cm and the member length is shorter than the designed value, the amplitudes of mode components in the first ring decrease and those in the second ring increase gradually. A zigzag pattern appears in the second ring. The amplitude of mode in the second ring is almost equal to that in the first ring. But, when the SD of the member length error is equal to 0.1 cm, the amplitudes of crown node and nodes in the first ring are on the same order. The amplitudes of nodes in the second ring are about one half those in the dome crown.

5. Conclusions

This study examined a single layer three-way pin-jointed grid shell of a wooden prefabricated truss system under uniform nodal gravity load. The member length error was focused among the imperfections in the prefabricated wooden truss system. The effect of the member length error on the initial imperfection and the nodal buckling behavior were shown statistically with the numerical calculations considering the geometrical nonlinearity. The main conclusions are as follows.

1) The mean of the initial axial forces on a member in the inner region is not clearly affected by the mean of the member length error. The mean of the initial axial force on a member in the peripheral region is affected by the sign and magnitude of the member length error. It is confirmed that the SD (standard deviation) of the initial axial force on a member varies almost linearly with the SD of the member length error, independently of the mean of the member length error.
2) It is confirmed that the mean and SD of the initial displacement of a node vary almost linearly with the mean of the member length error.
3) The mean of the nodal buckling load decreases as the SD of the member length error increases. The effect of the SD of member length error on the buckling load is larger than that of the mean of the member length error on the buckling load.
4) The one nodal buckling mode is most common in cases with a large SD of the member length error. The nodal buckling mode appears in the crown and the first ring. With small SD of member length error, the nodal buckling mode appears in the crown, first ring nodes and second ring nodes.

References

[1] AIJ, Stability analysis of single layer latticed domes, State-of- the art, Heki K. (ed.), 1989 (in Japanese).

[2] AIJ, Recommendation for quality criteria and inspection standards of steel structures, 2007 (in Japanese).

[3] Fujimoto M., Imai K., and Saka T., Numerical simulation of the buckling experiments of single-layer grid dome prestressed by PC bar, *Proceedings of the Conf. on Computational Engineering and Science*, Vol.3, 1998.5, pp.793-756 (in Japanese).

[4] Fujimoto M., Imai K., Furukawa T., Kusunoki M. and Ikemoto, M. , Experimental study of single layer two-way grid cylindrical shell roof composed of KiT-wood

space truss system with round timber, *Proceedings of IASS-APCS 2003 symposium Taipei*, Oct. 22-25, 2003.10.

[5] Fujimoto M., Imai K., Furukawa T. and Ikemoto M. ,Experimental study of single layer three-way grid dome composed of KiT-wood space truss system with round timber, *Proceedings of IASS 2004 Symposium Montpellier*, Sept. 20-24, TP102, 2004.9.

[6] Fujimoto M., Imai K., Ikemoto M., Machinaga T. and Kushima, S. ,Experimental study of single layer two-way grid dome composed of Kitruss wooden space truss system with PC bar as diagonal members, *Proceedings of IASS 2005 Symposium Romania*, Sept. 6-10, 2005.9, pp. 667-674.

[7] Fujimoto M., Ikemoto M., Imai K. and Machinaga T., Experimental study on 4-strut model tensegrity composed of the truss system with round timber and PC bar - beamlike structure -, *Proceedings of IASS APCS2006 Symposium Beijing*, Oct. 16-19, TE03, 2006.10.

[8] Fujimoto M., Machinaga T., Kaname T., and Imai K., Experimental study on archlike tensegrity structure of trapezoidal 4-strut model composed of the wooden truss system and PC bar, *Proceedings of IASS 2007 Symposium Venice*, Dec. 3-6, 2007.12.

[9] Fujimoto M., Kaname T., Imai K., Takino A., and Zhang Z., Experimental Study on Translational Dome Tensegrity Structure Composed of Wooden Truss System and PC Bar, *Proceedings of IASS SLTE 2008 Symposium Acapulc*o, Oct. 27-31, 2008.10.

[10] Kato S. and Muto I., On a method for estimation of an initial geometrical imperfection in single layer latticed dome, *Journal of Struct. Constr. Eng, AIJ*, No. 423, May, 1991, pp. 127-136 (in Japanese).

[11] Ogawa T., and Kuwada M., The estimation of elasto-plastic buckling load of rigidly jointed single-layer latticed domes, *Proceedings of the IASS 40th Anniversary Congress, Madrid*, Sept. 20-24, Vol. I, B2, 1-10, 1999